Lawrence Berkeley Laboratory
UNIVERSITY OF CALIFORNIA
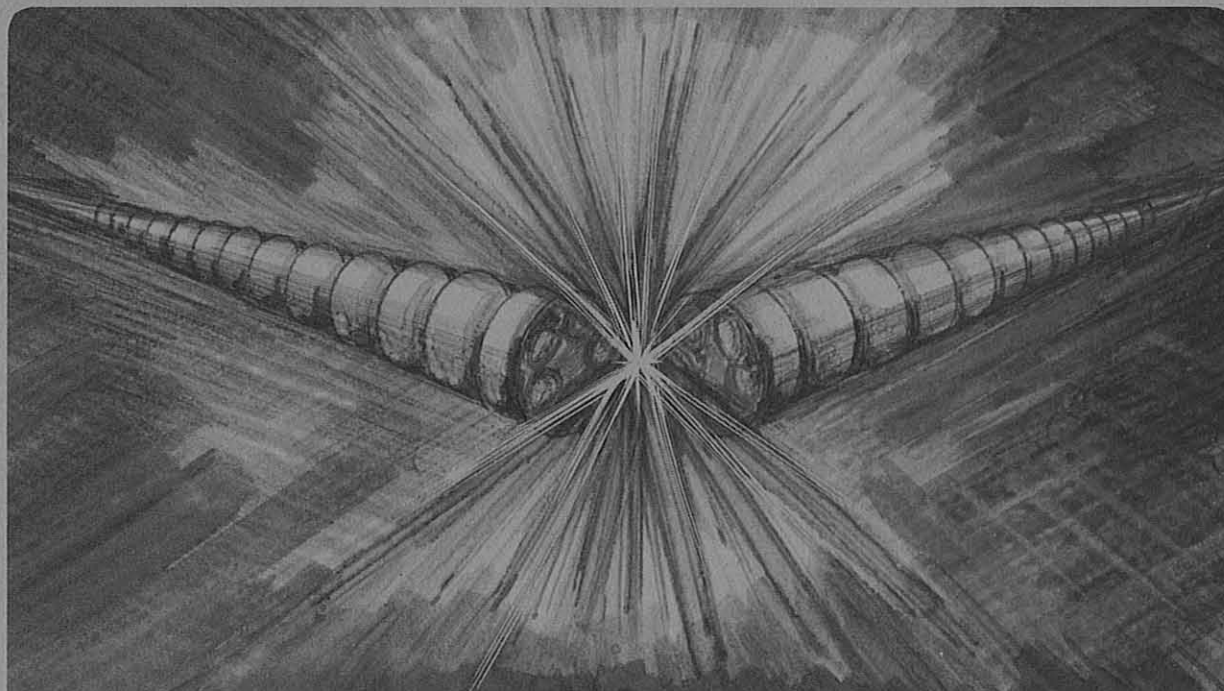
Accelerator & Fusion Research Division

Double RF System for Bunch Shortening

Y.H. Chin

November 1990

Double RF System for Bunch Shortening*

Yong Ho Chin

Accelerator and Fusion Research Division
Lawrence Berkeley Laboratory
1 Cyclotron Road
Berkeley, CA 94720

November 1990

Double RF System for Bunch Shortening*

Yong Ho Chin

Exploratory Studies Group
Accelerator & Fusion Research Division
Lawrence Berkeley Laboratory, Berkeley, CA 94720

I. Introduction

Present designs of high luminosity storage ring colliders, such as a B-Factory, employ small beta functions of $\beta^* \approx 1$ cm at the interaction point (IP) in order to achieve the required luminosity of 3×10^{33} cm^{-2}s^{-1} or more.[1] However, effective utilization of a small β^* requires a small bunch length, σ_z, as well, since the luminosity degrades unless $\sigma_z \leq \beta^*$. Taking into account bunch lengthening due to the microwave instability, a bunch length of $\sigma_z = 0.5 \sim 1$ cm is typically considered. Such a short bunch may be realized through using a high rf voltage and/or a high frequency, or by designing a ring with a low momentum compaction factor. There are some disadvantages with either of these approaches. For example, using a high rf voltage increases the rf power and may increase the required number of rf cavities as well. Such an increase in the number of rf cavities is generally undesirable because it increases the number and strength of parasitic higher-order modes that are the main source of coupled-bunch instabilities. Similarly, a ring with a very low momentum compaction factor is not a preferable choice, either.[2] This approach reduces the threshold bunch current for the microwave instability and the transverse mode-coupling instability (since the synchrotron tune will be reduced). If the required bunch current is larger than the threshold value of the microwave instability, the bunch will be lengthened (and its energy spread increased) so that we may fail to maintain the required bunch parameters. Depending on how it is varied, a change of the momentum compaction factor also affects the beam emittances.

A higher rf voltage helps shorten the bunch because it provides a steeper slope of the rf wave at the synchronous phase, and thus a deeper rf potential for the beam. The equivalent slope can also be obtained by using a higher-frequency rf system with angular frequency $n \cdot \omega_{rf}$ where ω_{rf} is the angular frequency of the original rf system. Then, the

1

required rf voltage is reduced to $1/n$ times the original voltage. However, high-power CW klystrons must be sought to feed power to these high-frequency cavities. Moreover, the momentum acceptance of the higher-harmonic rf system, which is proportional to $\sqrt{V_p/h}$ (the definitions are given below), may become too small.

It was suggested by Zisman that the combination of the two systems (double rf system) may be more effective to shorten a bunch, compromising between the desirable and the undesirable effects mentioned above. In this paper, we demonstrate (using the high energy ring of APIARY-VI as an example) that a double rf system is, in fact, quite effective in optimizing the rf performance. In Section II, the parameters used are explained, and some handy formulae for bunch parameters are derived. In Section III, we consider an example of bunch shortening by adding a higher-harmonic rf system to the main rf system. The parameters of the main rf system are unchanged. The double rf system, however, can be used for another purpose. Namely, the original bunch length can be obtained with a main rf voltage substantially lower than for a single rf system without necessitating a high-power source for the higher-harmonic cavities (a low-power source is generally still needed). Using a double rf system, the momentum acceptance remains large enough for ample beam lifetime. Moreover, the increase in nonlinearity of the rf waveform increases the synchrotron tune spread, which potentially helps a beam to be stabilized against longitudinal coupled-bunch instabilities. We will show some examples of this application in Section IV. In Section V, we discuss the choice of the higher-harmonic frequency. Our conclusions are presented in Section VI.

II. Double RF System

In this section, we define some quantities to describe the double rf system and then derive some useful formulae. The voltage seen by beam particles for the double rf system case is defined by

$$V(\phi) = V_p[\sin(\phi + \phi_s) + k\sin(n\phi + n\phi_n)], \tag{1}$$

where

$$
\begin{aligned}
V_p &= \text{peak voltage of the main rf system} \\
kV_p &= \text{peak voltage of the higher-harmonic rf system} \\
h &= \text{harmonic number of the main rf system} \\
n \cdot h &= \text{harmonic number of the higher-harmonic rf system} \\
\phi_s &= \text{synchronous phase angle of the main rf system} \\
n \cdot \phi_n &= \text{synchronous phase angle of the higher-harmonic rf system.}
\end{aligned}
$$

2

The Hamiltonian for synchrotron motion is given by

$$H = \frac{h\eta\omega_0^2}{2E_0\beta^2}W^2 + \frac{eV_p}{2\pi}U(\phi),$$ (2)

where

$$W = \frac{\Delta E}{\omega_0},$$ (3)

and

$$U(\phi) = -\frac{1}{V_p}\int_0^\phi (V(\phi) - V(0))d\phi.$$ (4)

The other parameters are as follows:

$$
\begin{aligned}
\omega_0 &= \text{angular revolution frequency} \\
\eta &= \alpha - 1/\gamma^2 = \text{phase slip factor} \\
\alpha &= \text{momentum compaction factor} \\
\gamma &= \text{Lorentz factor} \\
\beta &= \sqrt{1 - 1/\gamma^2} \\
E &= \Delta E + E_0 = \text{particle energy} \\
E_0 &= \text{energy of the synchronous particle} \\
e &= \text{elementary charge.}
\end{aligned}
$$

The quantity $eV(0)$ represents the synchrotron radiation loss per turn that must be replenished by the rf system.

The quantities k and ϕ_n are free parameters. However, for a given k, the shortest bunch can be obtained when

$$n\phi_n = \pi$$ (5)

since the slope of the higher-harmonic rf voltage reaches its negative maximum there. Using the condition expressed by Eq. (5) has several advantages. First, the higher-harmonic rf system provides the most linear voltage over the widest range of ϕ with this condition. Therefore, the rf potential will be least distorted from a parabolic shape. Second, the higher-harmonic system provides no acceleration to synchronous particles. Therefore, the higher-harmonic cavities need, in principle, only a small amount of power to compensate beam loading and the power loss in the cavity walls. Another advantage is that the voltage and the synchronous phase of the main rf system, V_p and ϕ_s, remain unchanged from the single rf system. To shorten or restore the bunch length, we just have to switch on and off the higher-harmonic rf system. For these obvious advantages, we set $n\phi_n$ to π in what follows.

Let us derive some useful formulae to characterize a beam in the double rf system. The unstable fixed point (in phase angle) ϕ_{sep} that defines the separatrix in phase space is given by a non-trivial($\phi \neq 0$) solution of

$$\sin(\phi + \phi_s) - \sin\phi_s - k\sin n\phi = 0. \tag{6}$$

The extrema of W corresponding to the separatrix are given by

$$W_{sep} = \sqrt{\frac{2E_0\beta^2}{h\eta\omega_0^2}\frac{eV_p}{2\pi}[\cos(\phi_{sep} + \phi_s) - \cos\phi_s + \phi_{sep}\sin\phi_s - \frac{k}{n}(\cos n\phi_{sep} - 1)]}, \tag{7}$$

or

$$\left(\frac{\Delta E}{E_0}\right)_{sep} = \sqrt{\frac{2\beta^2}{h\eta E_0}\frac{eV_p}{2\pi}[\cos(\phi_{sep} + \phi_s) - \cos\phi_s + \phi_{sep}\sin\phi_s - \frac{k}{n}(\cos n\phi_{sep} - 1)]}. \tag{8}$$

The above equation gives the momentum acceptance of the double rf system. Equation (8) can be rewritten using the synchrotron tune of the single rf system, Q_{s0}, as

$$\left(\frac{\Delta E}{E_0}\right)_{sep} = \frac{V_p}{2\pi Q_{s0}E_0}$$
$$\times \quad \sqrt{-2\cos\phi_s[\cos(\phi_{sep} + \phi_s) - \cos\phi_s + \phi_{sep}\sin\phi_s - \frac{k}{n}(\cos n\phi_{sep} - 1)]}. \tag{9}$$

The equilibrium beam profile is given by

$$I(\phi) = K \cdot \exp\{\frac{1}{\sigma_{\phi 0}^2\cos\phi_s}[\cos(\phi + \phi_s) - \cos\phi_s + \phi\sin\phi_s - \frac{n}{k}(\cos n\phi - 1)]\}, \tag{10}$$

where

$$\sigma_{\phi 0} = \frac{2\pi h}{C}\sigma_{z0}, \tag{11}$$

and $\sigma_{\phi 0}$ and σ_{z0} are the bunch length in the single rf system measured in rf phase and in the longitudinal distance from the bunch center, respectively, C is the ring circumference, and K is the normalization constant. The two variables ϕ and z are related to each other by the same relationship as $\sigma_{\phi 0}$ and σ_{z0}, as specified in Eq. (11). The bunch length σ_z in the double rf system is obtained by expanding trigonometric functions in Eq. (10) by Taylor series around the bunch center. We have

$$\sigma_z = \sigma_{z0}/\sqrt{1 - \frac{nk}{\cos\phi_s}}. \tag{12}$$

Note that since $\cos\phi_s \cong -1$, the argument of the square root is always larger than 1, that is, $\sigma_z \leq \sigma_{z0}$. The synchrotron tune Q_s of the double rf system at small amplitude in phase space is calculated in a similar way, and is given by

$$Q_s = Q_{s0}\sqrt{1 - \frac{nk}{\cos\phi_s}}. \tag{13}$$

It is interesting to note that the product of the bunch length and the synchrotron tune is preserved in the two systems:

$$\sigma_z \cdot Q_s = \sigma_{z0} \cdot Q_{s0}. \tag{14}$$

III.   An Example of Bunch Shortening

Here we consider an example of bunch shortening using a higher-harmonic rf system with $n = 2$ and $k = 0.5$. Figure 1 shows the rf voltages of the single rf system and the double rf system, labelled by "S" and "D", respectively. The parameters used are relevant to the high energy ring of APIARY-VI. They are listed in Table 1.

Table 1.   Parameters of the high energy ring of APIARY-VI used for the bunch shortening example.

Circumference, C (m)	2200
Beam energy, E_0 (GeV)	9.0
Momentum compaction factor, α	0.00245
Harmonic number of the single rf system, h	3492
Rms bunch length in the single rf system, σ_{z0} (cm)	1.0
Rms relative energy spread in the single rf system, $\frac{\sigma_E}{E_0}$	0.0006
Rms phase spread in the single rf system, $\sigma_{\phi 0}$ (rad)	0.1
Momentum acceptance of the single rf system, $\left(\frac{\Delta E}{E_0}\right)_{sep}$	0.0105
Synchrotron tune of the single rf system, Q_{s0}	0.0523
Peak voltage of the single (& main) rf system, V_p (MV)	18.5
Synchronous phase of the single (& main) rf system, ϕ_s (deg)	169.03
Ratio of the higher-harmonic frequency to the main frequency, n	2
Ratio of the higher-harmonic rf voltage to the main rf voltage, k	0.5
Synchronous phase of the higher-harmonic rf system, ϕ_n (deg)	90.0

The rf potentials are plotted in Fig. 2. Figure 3 shows the separatrices in longitudinal phase space. The momentum acceptance of the double rf system is slightly enlarged to 0.0112 from $\left(\frac{\Delta E}{E_0}\right)_{sep} = 0.0105$ of the single rf system, while the phase acceptance is reduced. Both acceptances are large enough for ample beam lifetime in the two rf scenarios. Needless to say, the choice of the rf system does not affect the energy spread of a beam. The beam profiles as a function of the longitudinal distance, z, are plotted in Fig. 4 in units of the bunch length of the single rf system, σ_{z0}. The calculated value of the rms bunch length from Eq. (12) is 0.704 cm, while the computed value from Fig. 4 is 0.706 cm. They are in good agreement. Figure 5 shows the same beam profile on a logarithmic scale. The small difference of the beam intensity at $z = \pm 10\sigma_{z0}$ is due to the small asymmetry of the rf potential (see Fig. 2). Figure 6 shows the synchrotron tune, Q_s, as a function of z normalized by σ_{z0} where the particle trajectory and the positive longitudinal axis intersect. One can see that Q_s drops at a faster rate with z than in the case of the single rf system. The resulting larger tune spread may help to stabilize longitudinal beam instabilities.

IV. Reduction of the Main RF Voltage

In the previous section, we considered the example of bunch shortening by adding a higher-harmonic rf system to the main rf system. The voltage of the main rf system remained unchanged in that example. The double rf system, however, can also be used for another purpose. Namely, the same bunch length can be achieved for a reduced voltage of the main rf system. This application is particularly beneficial if one wants to decrease the number of rf cavities to lower the HOM impedance and thus weaken coupled-bunch instabilities, provided that the reduction of impedance of the main rf system dominates the additional contribution of the higher-harmonic cavities to the impedance. A potential problem is that the momentum acceptance is reduced if the voltage of the main rf system is reduced. As seen in Fig. 3, however, the higher-harmonic rf system tends to increase the momentum acceptance as compared to the (reduced-voltage) single rf system. Therefore, the actual momentum acceptance will not be as low as it would be for the reduced-voltage single rf system by itself. We have taken $n = 2$ and studied three different values of k to indicate the range of possibilities. The rf parameters and the momentum acceptances are summarized in Table 2. Other parameters not listed are taken from Table 1.

Table 2.   Rf parameters and momentum acceptances for $n = 2$ and different values of k.

k	0	0.333	0.5	0.75
ϕ_s (deg)	169.03	161.75	158.06	152.44
V_p (MV)	18.5	11.24	9.42	7.61
$(\frac{\Delta E}{E_0})_{sep}$	0.0105	0.0078	0.0072	0.0067

The phase ϕ_s of the main rf system is given by

$$\tan \phi_s = \frac{\tan \phi_{s0}}{1 - \epsilon^2}[1 + \sqrt{1 - (1 - \epsilon^2)(1 - n^2 k^2)}], \tag{15}$$

where

$$\epsilon = n \cdot k \cdot \tan \phi_{s0} \tag{16}$$

and ϕ_{s0} is the synchronous phase of the original single rf system (i.e., the $k = 0$ case in Table 2). Since $\tan \phi_{s0} \approx 0$, Eq. (15) can be approximated by

$$\tan \phi_s \approx \tan \phi_{s0}(1 + nk). \tag{17}$$

The necessary voltage of the main rf system is given by

$$V_p = V_{p0}\frac{\sin \phi_{s0}}{\sin \phi_s} \approx V_{p0}\frac{1}{1 + nk}, \tag{18}$$

where V_{p0} is the voltage of the original single rf system.

The separatrices in phase space for the three values of k are plotted in Figs. 7, 8 and 9, respectively. In each figure, the separatrices of the original single rf system ($k=0$), the double rf system when the higher-harmonic system is turned off, and the double rf system when the higher-harmonic rf system is turned on, are denoted by "S", "M" and "D", respectively. One can see that the double rf system tends to make up some of the decrease of the momentum acceptance due to the reduction of the main rf voltage so that the momentum acceptance has a weak dependence of k and V_p. In all three cases, the momentum acceptance is still larger than 10 times the rms relative energy spread. Figure 10 shows the beam profiles on a logarithmic scale as a function of z in units of the rms bunch length of the single rf system, σ_{z0}, for the $k = 0.5$ case. The beam profile of the double rf system deviates slightly from that of the single rf system in the beam tail. The beam profiles for other k values look almost the same as Fig. 10.

V. Choice of Higher-Harmonic Frequency

From Eqs. (12) and (18), we notice that the bunch length and the peak main rf voltage remain nearly constant as n and k are changed while their product, $n \cdot k$, is kept fixed (remember that $\cos \phi_s \approx -1$). Obviously, a larger value for n is beneficial in reducing k. However, the nonlinear region of the higher-harmonic rf voltage approaches the bucket center as n increases, leading to further distortion of the particle motion compared with that of the single rf system. This may result in intolerably small momentum acceptance. At the same time, the nonlinearity of the rf voltage will increase particle population in the tail. Figures 11, 12 and 13 illustrate these problems. Figure 11 shows the separatrices for $n = 3$ and $k = 0.333$ which provides the same bunch length and the same voltage of the main rf system as the $n = 2, k = 0.5$ case of Section IV. (The notation follows that of Section IV.) As can be seen, the momentum acceptance is reduced to $\left(\frac{\Delta E}{E_0}\right)_{sep} = 0.0064$ from $\left(\frac{\Delta E}{E_0}\right)_{sep} = 0.0072$ for the $n = 2, k = 0.5$ case. The separatrix has now the shape of a gourd instead of a fish. The phase acceptance, on the other hand, is enlarged compared with that for the $n = 2, k = 0.5$ case in this particular example. Figure 12 shows the beam profiles on a logarithmic scale. Comparing with Fig. 10, it can be seen that the particle population increases in the tail.

Now let us increase k to reduce the main rf voltage further. Figure 13 shows the rf potential for the $n = 3, k = 0.5$ case which provides the same bunch length and main rf voltage as the $n = 2, k = 0.75$ case of Section IV. One can see that the potential has developed a local minimum around $\phi = -2$. The local minimum is caused by the superposition of the bottom peak of the higher-harmonic rf voltage on the top peak of the main rf voltage. Particles that escape from the beam core by quantum excitation or other mechanisms can and will be trapped in this local minimum. This trapping enhances the particle population in the beam tail, leading to very short beam lifetime. The bucket size also becomes too small. The rf parameters and the momentum acceptance of the above two cases are summarized in Table 3. Other parameters not listed are taken from Table 1. For $n = 2$, the local minimum does not appear for any k value.

Table 3.   Rf parameters and momentum acceptances for $n = 3$ and different values of k.

k	0	0.333	0.5
ϕ_s (deg)	169.03	158.07	152.44
V_p (MV)	18.5	9.42	7.61
$\left(\frac{\Delta E}{E_0}\right)_{sep}$	0.0105	0.0064	0.0050

The value of k where the local minimum starts to appear on the left hilltop of the potential well is a function only of the synchronous phase of the main rf system, ϕ_{s0}. Figure 14 shows this dependence. The curve can be interpreted as the absolute upper limit of k. Even with k below this curve, of course, the momentum acceptance may be too small.

From the specific examples shown above, we cannot derive any definite conclusion about what n would be a good choice. That depends on other parameters and machine constraints. We must make a careful investigation of the choice of n on a case by case basis.

VI. Conclusions

We have seen that a double rf system is quite effective to optimize the rf performance of a high-luminosity collider. It can be used to shorten a bunch by simply adding the higher-harmonic rf system to the main rf system without changing the main rf parameters, or to maintain the bunch length when the main rf voltage is substantially reduced.

The double rf system idea has generally been proposed for lengthening the bunch.[3] In this application, the phase and the voltage of the higher-harmonic system are chosen such as to make the first and second derivatives of the total rf wave zero at the bunch center. Then, the rf potential becomes quartic in phase, which reduces the restoring force near the bunch center, with the result that the bunch lengthens. Both analytical studies[4] and experimental observations[5,6] show that the actual bunch shape is very sensitive to the phase error between the two rf systems. A small error of the phases leads to a drastic distortion of the bunch shape from a flat-top shape. Obviously, this is not the case for the bunch-shortening application. There is no essential constraint in the choice of phase and voltage of the higher-harmonic rf system. A small deviation of the higher-harmonic rf phase from its chosen value, say $n\phi_n = \pi$ as in this study, will lead to only a slight change in the bunch length.

Since the higher-harmonic cavities do not contribute to the compensation of the synchrotron radiation loss, they need only a relatively small amount of power for the resistive power loss at the cavity walls. This suggests a possibility that the higher-harmonic system may be "beam powered" by the beam-induced voltage due to the beam loading effect.[7] In this case, the external power source generates a certain voltage, say, V_1, only during initial operation, and then the beam-induced voltage provides the required higher-harmonic rf voltage together with V_1. The beam-induced voltage could be used, by suitable detuning, to provide V_1 for the next passage of a bunch. Including

the feasibility of this beam-powered system, a future study should be done on how much power can be saved by employing the double rf system.

Acknowledgments

The author would like to thank M. Zisman for suggesting this problem and helpful discussions and careful proofreading of the manuscript. He also would like to thank G. Lambertson for helpful discussions.

References

1. *Investigation of an Asymmetric B-Factory in the PEP Tunnel*, Lawrence Berkeley Laboratory Report LBL PUB-5263, March, 1990.

2. M. Zisman, SLAC Report ABC Note-12/LBL-ESG Tech. Note-148, August, 1990.

3. A. Hofmann and S. Myers, in *Proc. of the 11th Intl. Conf. on High Energy Accelerators*, CERN (Birkhäuser Verlag, Basel, 1980), p.610.; Y. H. Chin, Nucl. Inst. Methods, **215**, 501(1983).

4. W. R. Fowkes and P. B. Wilson, SLAC Report, SPEAR-209, January 1989.

5. J. M. Paterson, private communication.

6. T. Weiland, KEK Report, TRISTAN Design Note TN-84-007, May 1984.

7. W. Schnell, CERN Report, LEP 70/101, August 1978.
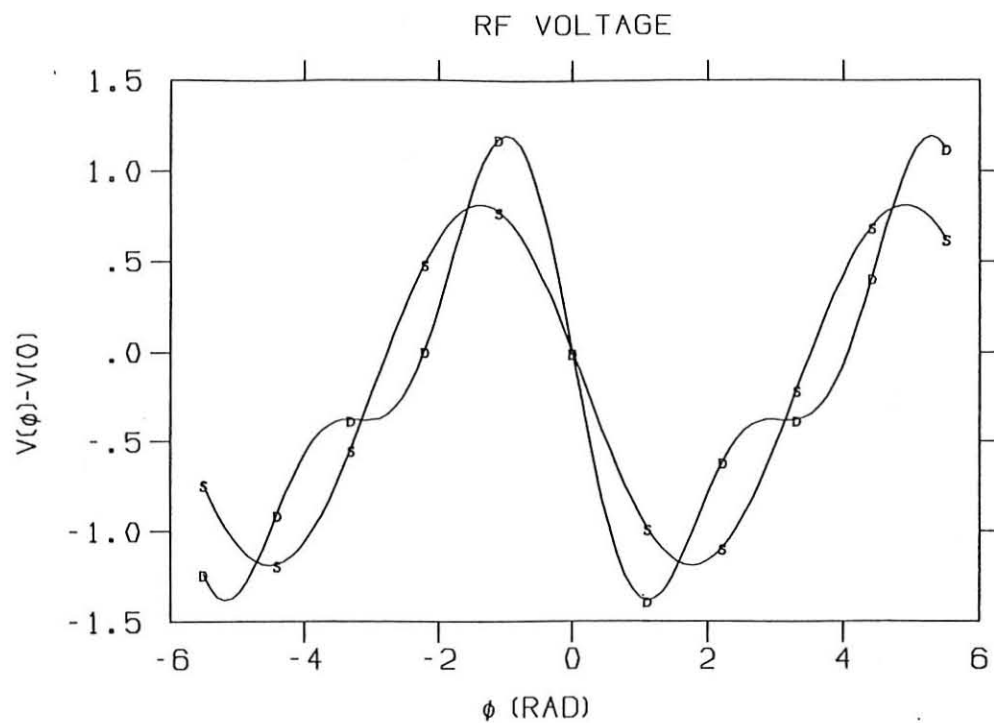
RF VOLTAGE

Figure 1: Voltages of the single and double ($n = 2, k = 0.5$) rf systems, labelled by "S" and "D", respectively.
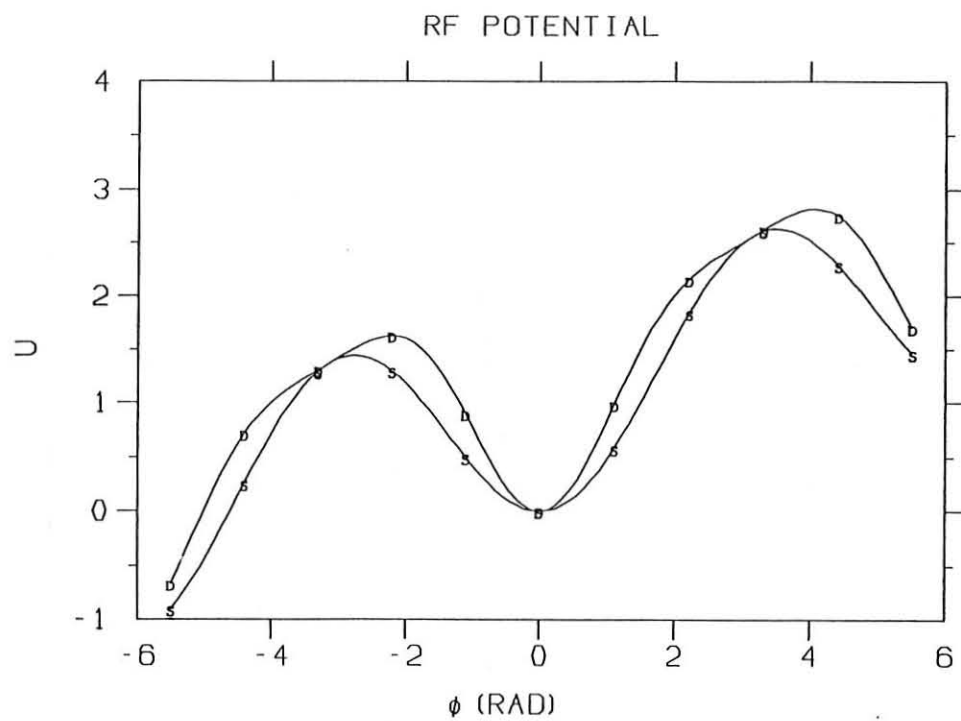
RF POTENTIAL

Figure 2: Rf potentials corresponding to Fig. 1.
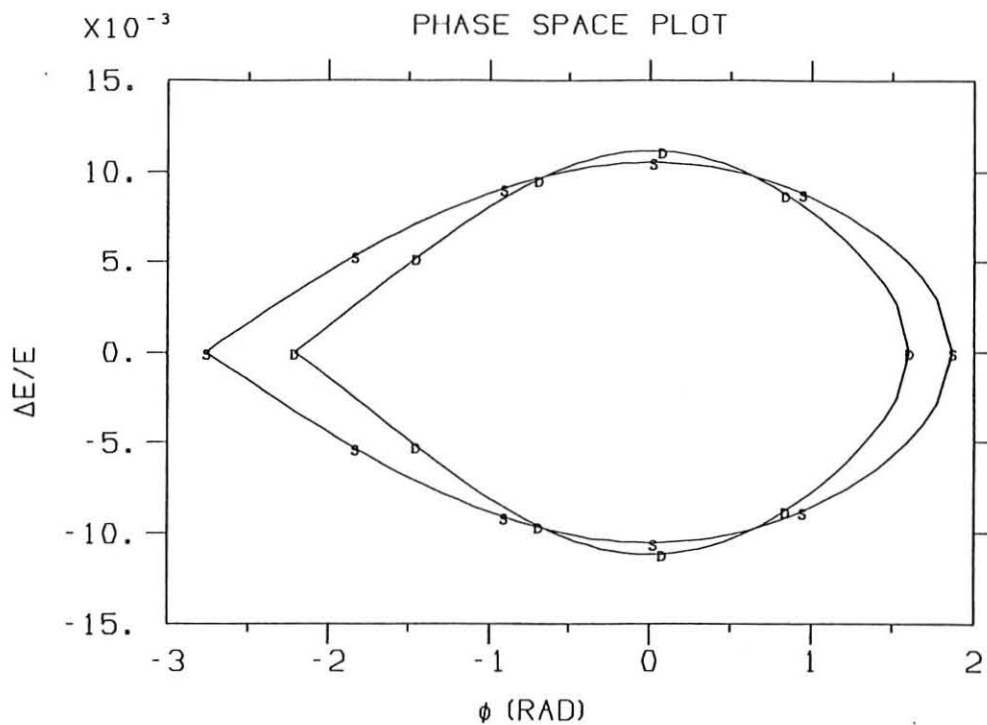
PHASE SPACE PLOT

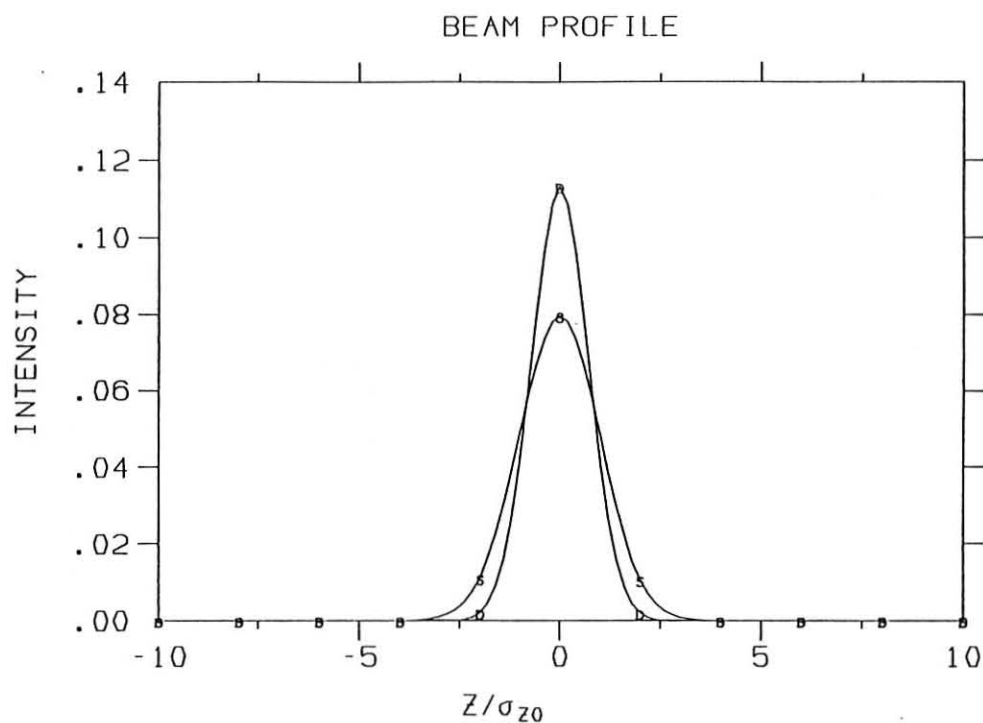Figure 3: Separatrices in longitudinal phase space for the cases in Fig. 1.

BEAM PROFILE

Figure 4: Beam profiles as a function of z (in units of σ_{z0}) on a linear scale, for the cases in Fig. 1.

BEAM PROFILE
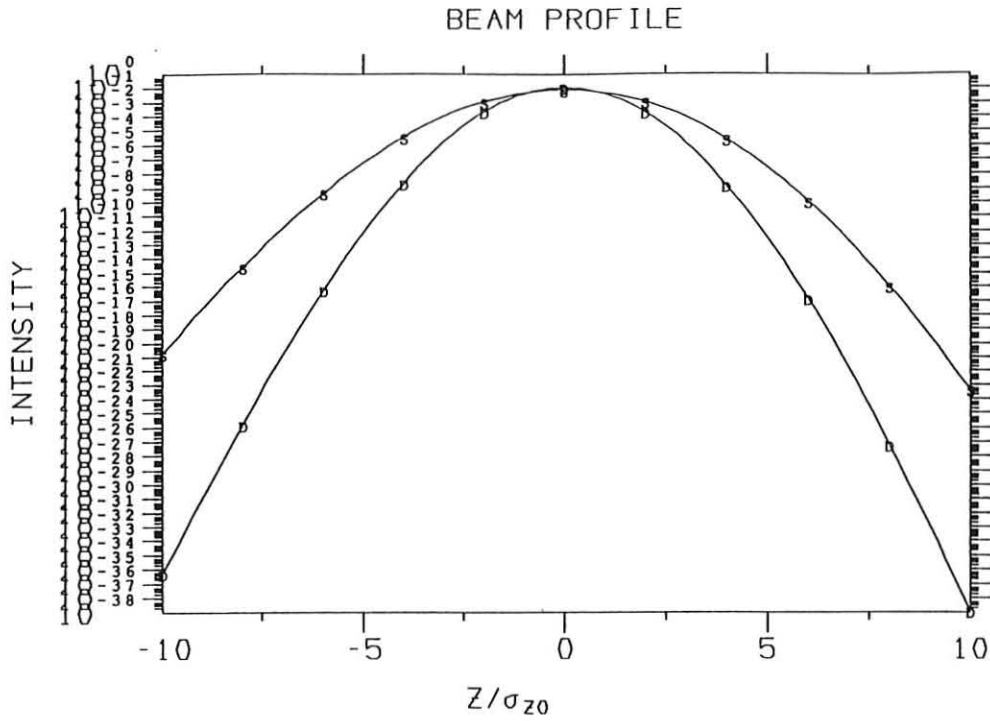
Figure 5: Same as Fig. 4, but using a logarithmic scale to emphasize the tails of the distributions.
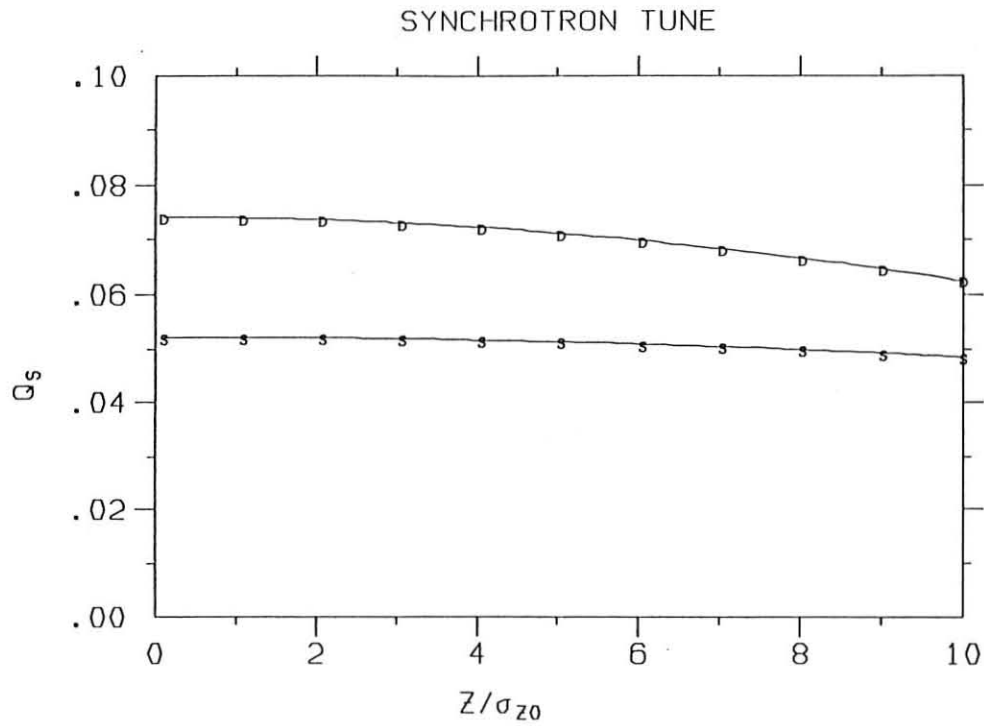
SYNCHROTRON TUNE

Figure 6: The synchrotron tune, Q_s, as a function of z (in units of σ_{z0}) for the cases in Fig. 1.

13
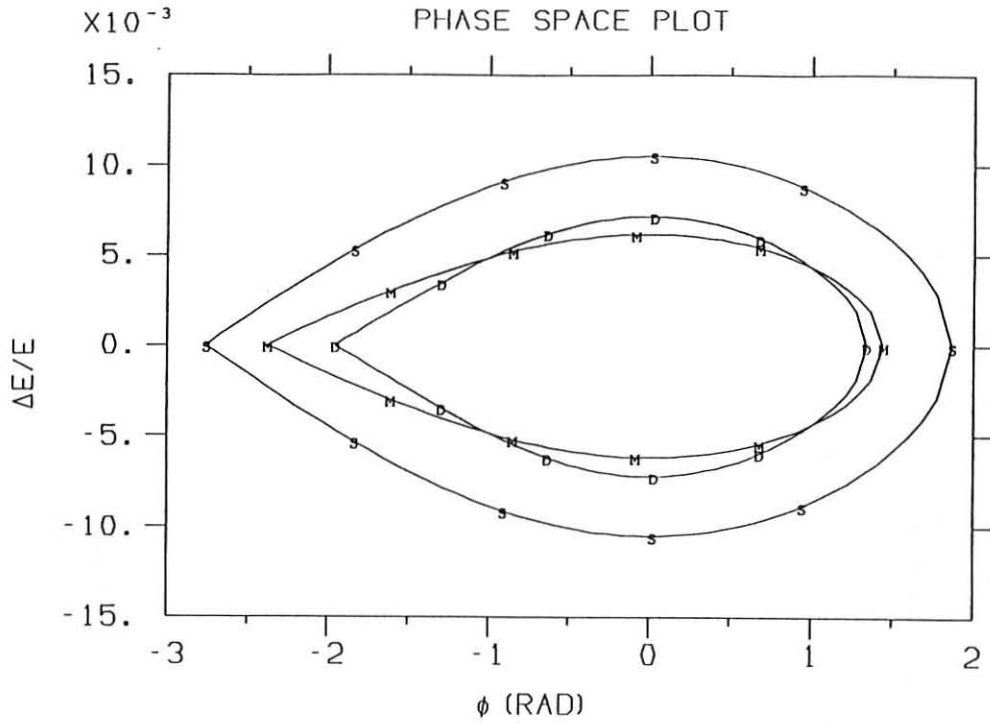
Figure 7: Separatrices in phase space for $n = 2$ and $k = 0.5$. "S" labels the original $(k = 0)$ single rf system, "M" denotes the reduced voltage operation of the main system not including the higher-harmonic voltage, and "D" denotes the full double rf system.
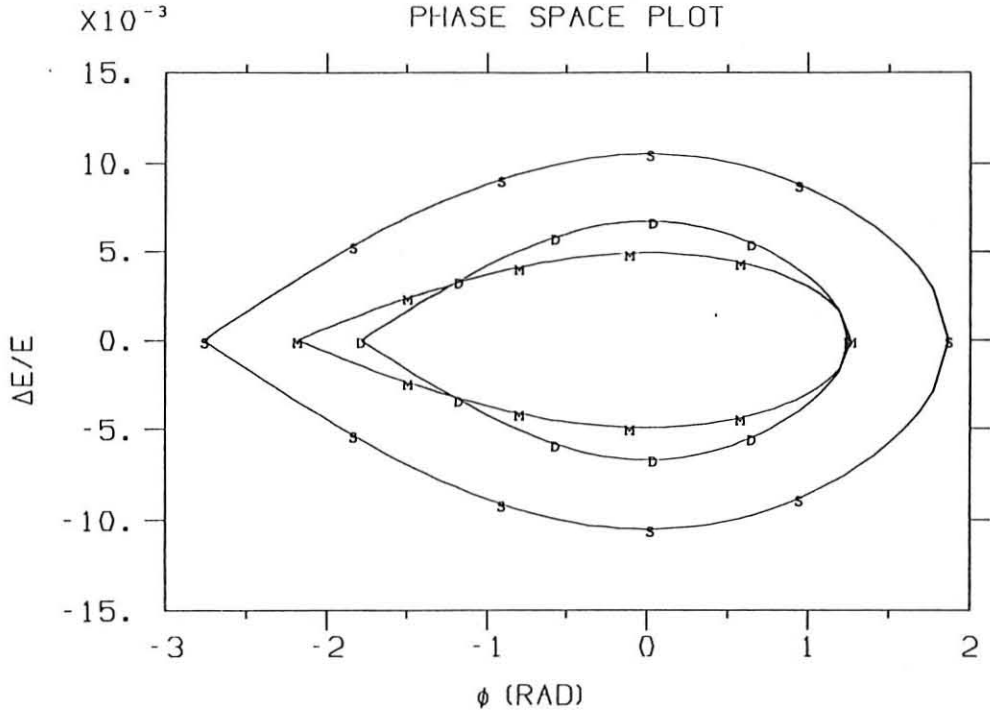
Figure 8: Separatrices in phase space for $n = 2$ and $k = 0.75$, using the same notation as in Fig. 7.

14
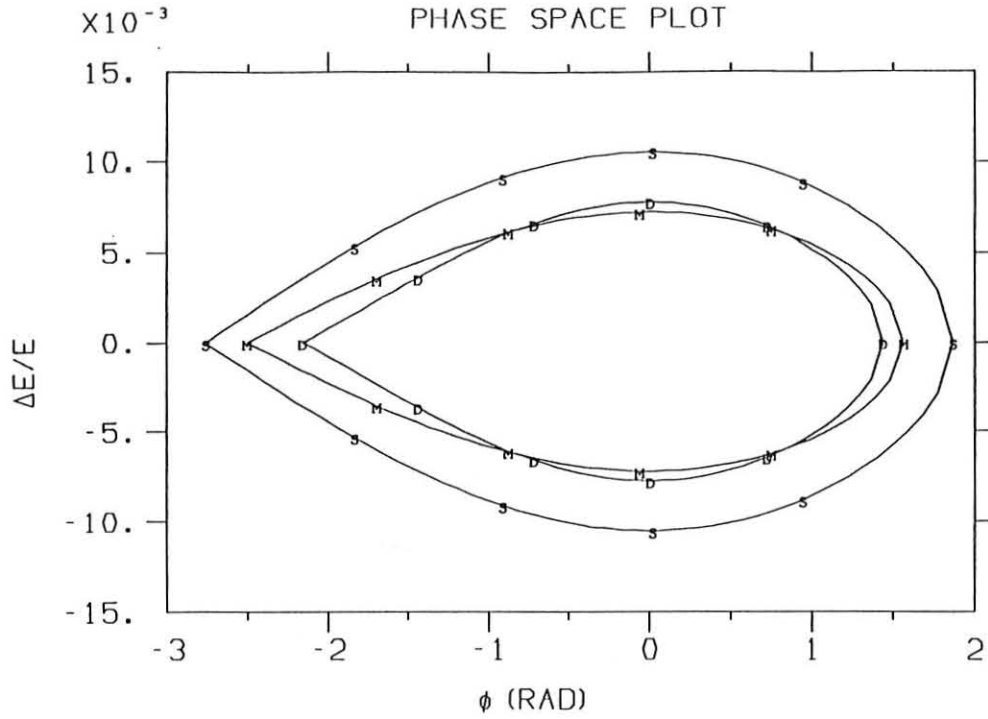
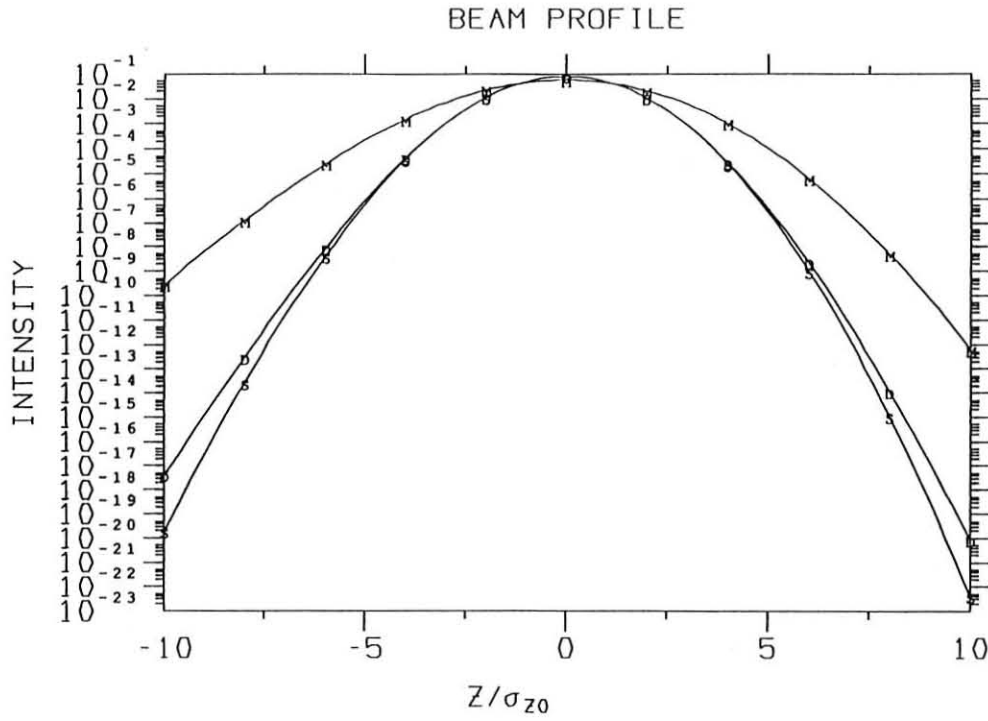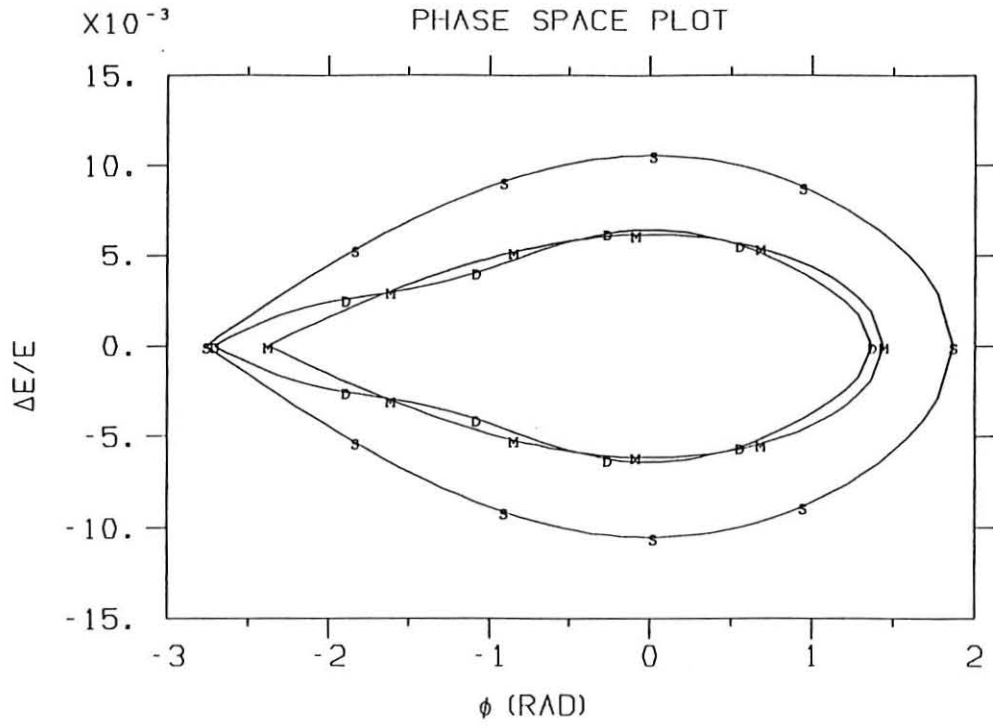Figure 9: Separatrices in phase space for $n = 2$ and $k = 0.333$, using the same notation as in Fig. 7.

Figure 10: Beam profiles on a logarithmic scale as a function of z (in units of σ_{z0}) for $n = 2$ and $k = 0.5$.

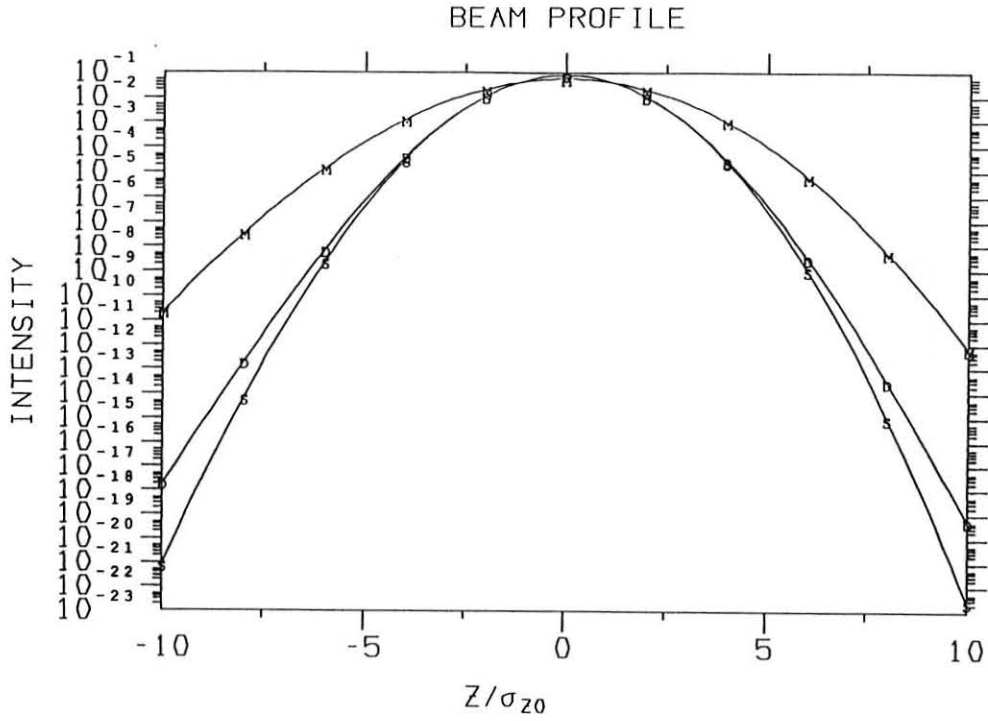Figure 11: Separatrices in phase space for $n = 3$ and $k = 0.333$, using the same notation as in Fig. 7.

Figure 12: Beam profiles on a logarithmic scale as a function of z (in units of σ_{z0}) for $n = 3$ and $k = 0.333$.
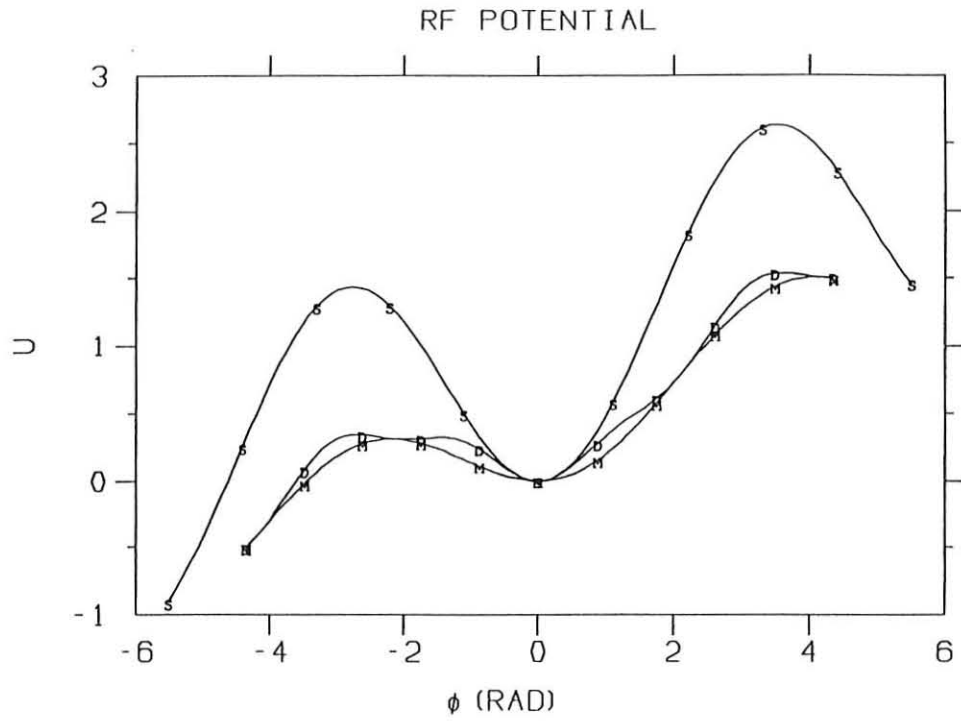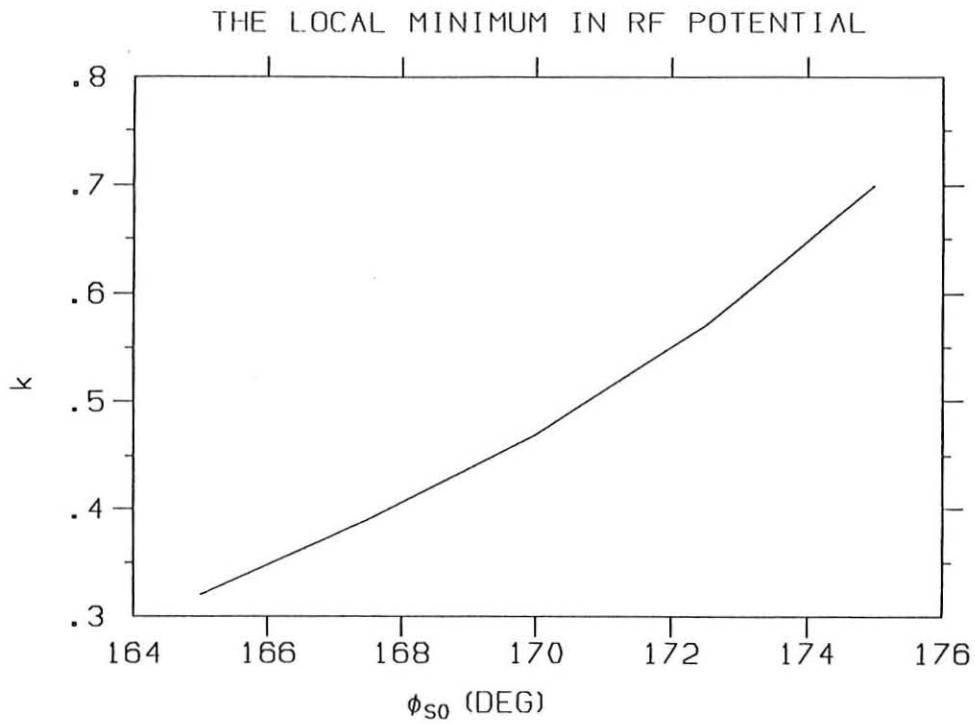
16

Figure 13: Rf potentials for $n = 3$ and $k = 0.5$.

Figure 14: The value of k where the local minimum starts to appear as a function of ϕ_{s0}.

17